
Microbial habitat dynamics and ablation control on the Ward Hunt Ice Shelf

Derek R. Mueller[†] and Warwick F. Vincent*

Centre d'études nordiques & Département de biologie, Université Laval, Québec, Canada

Abstract:

The Ward Hunt Ice Shelf (83°02'N, 74°00'W) is an ~40 m thick ice feature that occupies a large embayment along Canada's northernmost coast. Sediments cover 10% of its surface and provide a habitat for diverse microbial communities. These assemblages form an organo-sedimentary matrix (microbial mat) composed of cold-tolerant cyanobacteria and several other types of organisms. We investigated the environmental properties (temperature, irradiance, conductivity and nutrient concentration) of the microbial mat habitat and the effect of the microbial mats on the surface topography of the ice shelf. The low albedo of microbial mats relative to the surrounding snow and ice encouraged meltwater production, thereby extending the growth season to 61 days despite only 52 days with mean temperatures above 0 °C. We found large excursions in salinity near the microbial mat during freeze-up and melt, and 54% of all ponds sampled had conductivity profiles indicating stratification. Nutrient concentrations within the microbial mats were up to two orders of magnitude higher than those found in the water column, which underscores the differences between the microbial mat microenvironment and the overall bulk properties of the cryo-ecosystem. The average ice surface ablation in the microbial mat-rich study site was 1.22 m year⁻¹, two times higher than values measured in areas of the ice shelf where mats were less prevalent. We demonstrate with topographic surveys that the microbial mats promote differential ablation and conclude that the cohesive microbial aggregates trap and stabilize sediment, reduce albedo, and thereby influence the surface morphology of the ice shelf. Copyright © 2006 John Wiley & Sons, Ltd.

KEY WORDS Arctic; ice shelf; microbial mat; cryo-ecosystem; ablation; freeze concentration; microhabitat; inversion of relief

INTRODUCTION

Early explorers on the Greenland Ice Cap noted the presence of sediment and microbiota, and suggested that these communities could absorb heat and accelerate mass wasting. A. E. Nordenskjöld stated in 1870 that

in the above-mentioned powder, a brown polycellular alga, which, small as it is, together with the powder and certain other microscopic organisms by which it is accompanied, is the most dangerous enemy to the mass of ice, so many thousand feet in height and hundreds of miles in extent (Leslie, 1879).

Since that time many studies have noted that microbiota on or within ice cause reduced albedo and could thereby accelerate the melting of sea ice (Blanck *et al.*, 1932), river ice (Brandt, 1931) and glaciers (Adams, 1966; McIntyre, 1984; Takeuchi *et al.*, 1998; Fountain *et al.*, 2004), although direct tests of this biotic control of the physical environment are generally lacking.

A related 'inversion of relief hypothesis' was described anecdotally on ice islands (T-3 and ARLIS II) that calved from ice shelves along the northern coast of Ellesmere Island. Smith (1961) noted the dynamic nature of

* Correspondence to: Warwick F. Vincent, Département de biologie, Université Laval, Québec, QC G1K 7P4, Canada.

E-mail: warwick.vincent@bio.ulaval.ca

[†] Present address: Geophysical Institute, University of Alaska Fairbanks, Fairbanks, Alaska, USA.

their surface topography and described a cyclical development of surface forms in which differences in surface-cover albedo lead to successional reversals in relative surface elevations. These and related observations (Smith, 1964; Schraeder, 1968) suggested that depressions fill with water or snow, freeze-up over winter and that this ice remains resistant to ablation the following summer due to its relatively high albedo, with sediment acting as a driver of differential ablation. However, the underlying mechanism of ablation control has not been tested.

The Ward Hunt and Markham Ice Shelves (Figure 1) are the easternmost of five major ice shelves in the Canadian High Arctic. They were formed by the *in situ* accretion of marine and meteoric ice between 4500 and 3000 years ago (Jeffries, 2002). The accumulation of sediments on the surface of these ice shelves has provided a habitat for diverse consortia of microorganisms. These assemblages are dominated by filamentous oscillatorian cyanobacteria, but also contain diatoms, green algae and heterotrophic bacteria (Mueller *et al.*, 2005b) that, together, make up a loosely cohesive microbial mat. These microbiota tolerate the extreme conditions in their environment, including the combined stresses of high salinities and low water activity during winter and the high solar irradiance and near-freezing temperatures during the melt season (Mueller *et al.*, 2005a). Over large scales, ice shelves appear to be immutably frozen in time and space; yet, at the microhabitat scale, the physico-chemical environment is potentially dynamic. Spatio-temporal variations in irradiance, temperature, salinity and nutrient concentrations at the scale of the microbial mats have implications for the productivity and survival of microbiota. To date, there is a paucity of information regarding the environmental characteristics of microhabitats on Northern Hemisphere ice shelves, making it difficult to evaluate the limits to life in this extreme ecosystem. Although environmental conditions may impinge on biological activity on these ice shelves, it is also likely, as Nordenskjöld pointed out, that the microbiota have some capacity to influence the energy balance on the ice shelf and thereby alter the physical structure of their surroundings.

Our primary objectives in the present study were: (1) to define the physico-chemical environment of an ice shelf ecosystem at the scale of the microbial mats and to address the hypothesis that the microbiota exist in conditions that differ from those more generally found on the ice shelf; (2) to test the ‘inversion of relief’ hypothesis put forward by Smith (1961) with quantitative survey and ablation data from two consecutive summers on the Ward Hunt Ice Shelf. We further developed this hypothesis by considering that the microbial mat exerts a stronger influence on the ice shelf ablation than do abiotic, inorganic sediments.

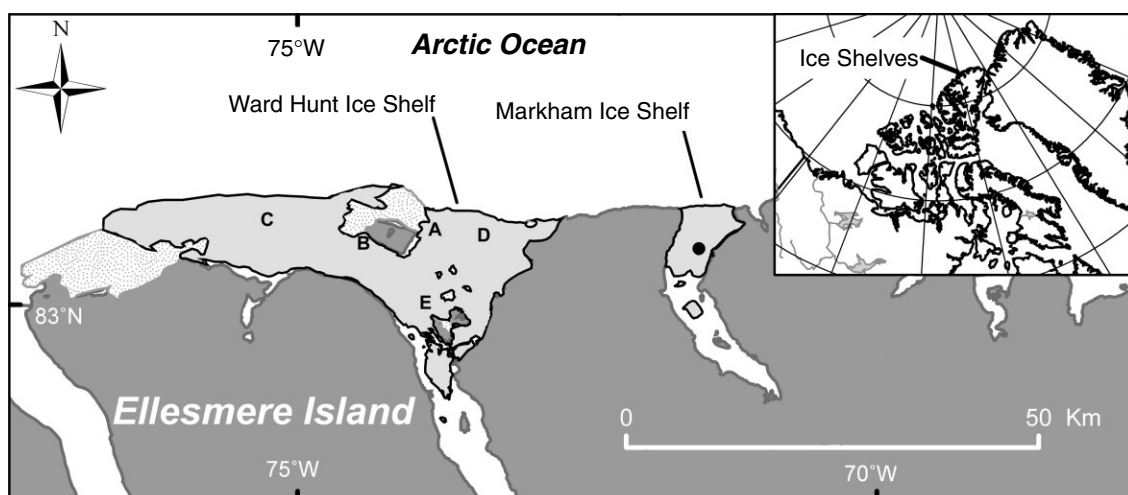


Figure 1. Location map of the Ward Hunt and Markham Ice Shelves. Data were collected in areas adjacent to the climate station (B) and in the centre of Markham Ice Shelf (black circle). The locations of ablation stake clusters are shown (letters A–E). Clusters B and E were in marine ice areas, whereas clusters A, C and D were in meteoric ice areas

METHODS

Study site

Our study sites were established in a marine ice area on the Ward Hunt Ice Shelf and on the Markham Ice Shelf (Figure 1). These areas have a high coverage of surface sediment and have thick, luxuriant microbial mats, often with an orange–red surface layer. The mats are found both underwater (benthic) and above the water line (emergent). Less-developed mats are also found in these locations and were often observed in cylindrical meltholes in the ice surface (cryoconite holes).

Microhabitat climate

An automated climate station for microhabitat environmental measurements was erected at the beginning of August 2001 at the Ward Hunt Ice Shelf study site ($83^{\circ}04.987'N$, $74^{\circ}25.277'W$; Figure 2). Climatological data were averaged hourly by a CR10X datalogger, which was later augmented by an AMT25 multiplexer (Campbell Scientific, Logan, UT). Key variables were air temperature (Campbell Scientific, 107 thermistor shielded with a six-plate Gill screen), downwelling photosynthetically active radiation (PAR), upwelling PAR (both LI-190SA Li-Cor, Inc., Lincoln, NE) and an underwater PARsensor (Li-Cor, LI-192SA) that was placed just above the microbial mat surface. During the summer field seasons of 2002 and 2003, an anemometer (RM Young, 05103-10) was also installed. The station's 3 m-long supports were periodically reinstalled to counteract ice ablation; therefore, instrument (radiometers, air temperature and anemometer) heights varied between 1.50 and 2.60 m above the ice shelf surface. During the summers of 2002 and 2003, the anemometer shadowed the radiometers (Figure 2c) at certain times of the day, necessitating the removal of affected data (~ 1 h per day).

To record dates of freeze-up and thaw plus temperature minima in microbial mats in areas adjacent to the climate station, thermistors (Omega 44033, Omega Engineering Inc., Stamford, CT) and self-contained temperature loggers (Stowaways, Onset Computer Corporation, Bourne, MA) were buried in microbial mats over winter. Microbial mat thermistor and Stowaway temperatures in a stirred ice bath agreed within $\pm 0.2^{\circ}C$ which surpassed their rated accuracy of $\pm 0.1^{\circ}C$ and $\pm 1.2^{\circ}C$ respectively.

In 2002, an XR-420 CTD datalogger (RBR Ltd, Ottawa, ON) was installed 1–2 cm above the surface of the microbial mat at the bottom of a meltwater pond at a depth of 42 cm and set to log temperature and

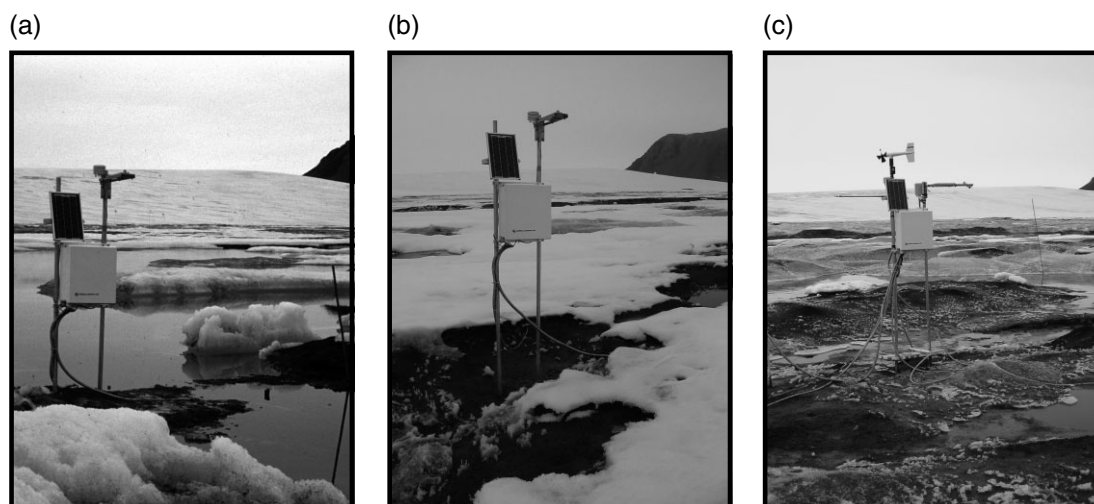


Figure 2. Photographs of the climate station in (a) August 2001, (b) July 2002 and (c) July 2003. Changes in cover type (snow, mat, ice and water) and inversion in topography can be clearly seen between each successive year. Note that there was considerable melt between mid July 2002 (b) and when the topographic survey was completed in late July (Figure 10b)

specific conductivity (specific to 25 °C) every 30 min. Two Stowaway temperature loggers were placed along a tether at depths of 20 and 30 cm between the CTD instrument and a post at the pond edge. These instruments were left in place over winter to record the progression of the freezing front and the change in pond water conductivity just above the microbial mat surface. The CTD temperature and conductivity accuracies were rated at ± 0.002 °C and ± 0.003 mS cm⁻¹ respectively.

Spot measurements of albedo were taken at 50, 100 and 150 cm above representative surfaces on the Markham and Ward Hunt Ice Shelves using a Li-Cor, LI-1400 datalogger and two LI-190SA PAR sensors mounted on a levelled rod. This setup was also used to obtain albedo values from a helicopter that flew over representative ice surfaces at a constant altitude of 130 m.

Water column and microbial mat profiles

Water column profiles of conductivity and temperature were taken using a portable instrument (pH/Con 10 Series, Oakton Instruments, Vernon Hills, IL). If present, ice cover was carefully removed to allow access while minimizing water column disturbance. A variety of small cryoconite holes to medium-sized meltponds on the Ward Hunt and Markham ice shelves were profiled at an interval of 5 to 10 cm. A stratification index was calculated by dividing the bottom water conductivity by the surface water conductivity to allow a direct comparison of the water column stratification between each profile.

Microbial mats were profiled using a DO-166-NP dissolved oxygen needle probe and a PHM-146 micro pH mono probe as well as an ISM-146 chloride-ion-selective microelectrode, with a DJM-146 micro double junction reference electrode (Lazar Research Laboratories Inc., Los Angeles, CA). Profiles commenced at the microbial mat surface in two types of microhabitat: a cryoconite hole with loosely cohesive mats overlain by 8 cm of water, and a thick emergent mat with an orange-pigmented surface layer that was saturated with water. For dissolved oxygen concentration it was assumed that microbial mats overlain by water were at 1 °C and mats not overlain by water were at 5 °C. The vertical spatial resolution of the probes was up to 0.4 mm, 0.3 mm and 1.5 mm for pH, chloride and dissolved oxygen respectively. The electrodes were lowered into the mat with a micromanipulator at intervals of 0.62 mm.

Nutrient concentrations and isotopic ratios

The meltwaters from several small ice shelf ponds and cryoconite holes with benthic microbial mats were sampled for nutrient analysis. These ponds were then pumped dry, the microbial mats were lifted out of the holes and gently compressed between two clean nesting plastic containers. Expressed microbial mat pore water was then collected for nutrient analysis (Vincent *et al.*, 1993; Villeneuve *et al.*, 2001). Microbial mats that were not overlain by water (emergent mats) were also sampled in the same manner. Nutrients (NH₄⁺-N, NO₃⁻-N, NO₂⁻-N, soluble reactive phosphorus (SRP), dissolved organic and inorganic carbon (DOC and DIC), total dissolved nitrogen (TDN) and total dissolved phosphorus (TDP) were determined from filtered (cellulose acetate, 0.2 µm) water samples by the National Laboratory for Environmental Testing (NLET), Burlington, ON, Canada. Methods included automatic colorimetry for total phosphorus (stannous chloride), SRP (ammonium molybdate–stannous chloride), total nitrogen and ammonium (indophenol) and nitrate/nitrite (cadmium reduction). DIC and DOC were determined by infrared gas analysis and by UV digestion followed by infrared gas analysis respectively. Sample water was also filtered through GC-50 filters (GF/C equivalent, AMD Manufacturing, Mississauga, ON) to remove particulates and the filtrate was preserved in amber glass bottles for chromophoric dissolved organic matter (CDOM) absorbance determinations at 320 nm by spectrophotometry on a Cary 300 Bio UV–Vis spectrophotometer (Varian, Mulgrave, Australia). The absorption coefficient of CDOM was calculated using the equation of Kirk (1983): $a_{\text{CDOM}} (\text{m}^{-1}) = 2.303(A_{320 \text{ nm}})/r$, where the CDOM is the absorption coefficient at 320 nm, $A_{320 \text{ nm}}$ is the absorbance at 320 nm and r is the path length of the measurement cell. CDOM fluorescence data were obtained using a Cary Eclipse spectrofluorometer with an excitation at 370 nm and emission wavelengths of 450 and 550 nm. Absorption at these wavelengths within the measurement cell was found to be negligible. The

McKnight ratio (fluorescence index) was calculated as the fluorescence at 450 nm divided by the fluorescence at 550 nm (McKnight *et al.*, 2001).

Microbial mats from a variety of small- to medium-sized cryoconite holes were sampled and frozen for transport to Quebec City. They were then acidified by fuming with 37% HCl, to remove inorganic carbon, lyophilized and analysed for carbon and nitrogen isotopes on an isotope ratio mass spectrometer (Fisons Instruments, model VG Prism Isotech) by Delta Lab, Geological Survey of Canada, Quebec City. Isotopic data were expressed in delta notation relative to standards of carbon (PeeDee Belemnite) and nitrogen (atmospheric nitrogen). As an index of sample heterogeneity and analytical error, triplicate analyses of two samples yielded standard errors of 0.14‰ and 0.05‰ for carbon and nitrogen respectively.

Ice ablation, snow cover and topographic surveys

In 2002, six ablation stakes were drilled into the ice surface surrounding the climate station. At each site visit, measurements were taken from the top of each pole to the ice surface, taking care to average out microtopographic variations in the ice. Ice ablation was converted to water equivalent (w. eq.) ablation by multiplying ice ablation by 0.9 (Braun *et al.*, 2004). Two thermocouple arrays with 10 cm spacing between thermocouples were placed in contrasting locations (a plateau and a hollow) to assess differences in overwinter snow depth using thermal response to determine snow-cover presence or absence.

The 26 m × 43 m area defined by the ablation stakes was surveyed, using a Wild-Heerbrugg T-1 optical theodolite and stadia rod, between 4 and 6 August 2002 and again on 27 and 28 July 2003. The tripod was relevelled repeatedly due to its melting into the ice, creating closure errors that were on the order of 10 cm horizontal and 1 cm vertical. Topographic data (138 points in 2002, 291 points in 2003) were placed in the same Cartesian coordinate system, using one of the ablation stakes as an arbitrary datum. Both the surfaces were gridded by linear kriging to 108 × 65 grid nodes (Surfer 7.0, Golden Software, Golden, CO) and the modelled 2003 surface was subtracted from the modelled 2002 surface to identify regions of greatest ablation and to calculate the total volume of ice lost. The modelled surfaces in both years resembled the overall topographic pattern; however, due to kriging interpolation and some undersurveyed areas, the surfaces do not accurately portray hydrological gradients. This was exacerbated by the ability of water to erode vertical slots into the ice. In this paper, we define surface lowering as the height difference between the 2003 ice surface and the 2002 ice surface. For the surveyed data, net ablation refers to the loss of water equivalent mass (assuming an ice density of 0.9 g cm⁻³) between these 2 years and accounts for the presence of liquid water in the pond, even though advective gains and losses were not monitored.

The dominant surface cover types (ice, microbial mat, snow and water) were mapped using survey notes and photographs and were recreated in ArcMap 8.0 (ESRI Inc., Redlands, CA) by digitizing polygons referenced to survey points. Note that this characterization does not provide information on subjacent cover types. For example, the surface cover type 'water' may refer to a pond with a benthic mat and/or a bare ice bottom. By 'snow' we mean a highly reflective surface crystalline layer, which may be derived from snowfall or from the candling of pond ice. The change in cover type between 2002 and 2003 at each grid node was also determined and these data were used as levels in a one-way analysis of variance (ANOVA) on ranks (data were not normally distributed) of cover type versus elevation at each grid node (SigmaStat, 3.0, SPSS Inc., Chicago).

In 2004, 30 ablation stakes were installed on the Ward Hunt Ice Shelf. The stakes were placed in clusters of six, 50–100 m apart at five locations (Figure 1). One of these clusters (B) was located near the climate station. Cluster A was located in a meteoric ice area (region where the surface exposed ice was derived from snow and/or rain) near stakes measured by Braun *et al.* (2004). Clusters C and D were located farther from land in meteoric ice areas whereas cluster E was located in a marine ice area in the southern portion of the Ward Hunt Ice Shelf. These stakes were remeasured in August 2005 following the methods described above. The interval between measurements was 362 days (clusters A and B) or 363 days (clusters C, D and E).

RESULTS

Microhabitat climate

A year-long (August 2001 to August 2002) comparison between air temperature and microbial mat temperatures indicated that all the microbial mats were encased in ice and/or snow through most of the year, since their temperatures were relatively constant and less extreme than air temperatures (Figure 3a). Overwinter mat temperatures were relatively stable, reaching an average minimum of -16.9°C ($\text{SE} = 0.46^{\circ}\text{C}$) during April 2002, whereas mean daily air temperatures fell to -44.5°C in February 2002 (Figure 3a). Dates of freeze-up and thaw for each instrumented microbial mat are given in Table I, and the freeze-up and thaw of one microbial mat in 2001–02 is shown in Figure 3b and c. Delays in mat freeze-up and thaw, relative to mean daily air temperatures, illustrate the thermal buffering effect of the high heat capacity and the latent heat of fusion for the water and snow/ice that envelop this ecosystem (Figure 3b and c). During summer months, this thermal buffering prevented mat temperatures from rising substantially above 0°C . In 2001–02, the microbial mats spent an average period of 300 days ($\text{SE} = 10.6$ days, $n = 3$) frozen over winter, which compares to an average frozen period of 317 days ($\text{SE} = 4.0$ days, $n = 7$) in 2002–03 (Table I). From these observations we inferred growing seasons (365 minus the number of days below 0°C) of 65 and 48 days. These inferences are reasonable given an observed melt period of 61 days in 2002.

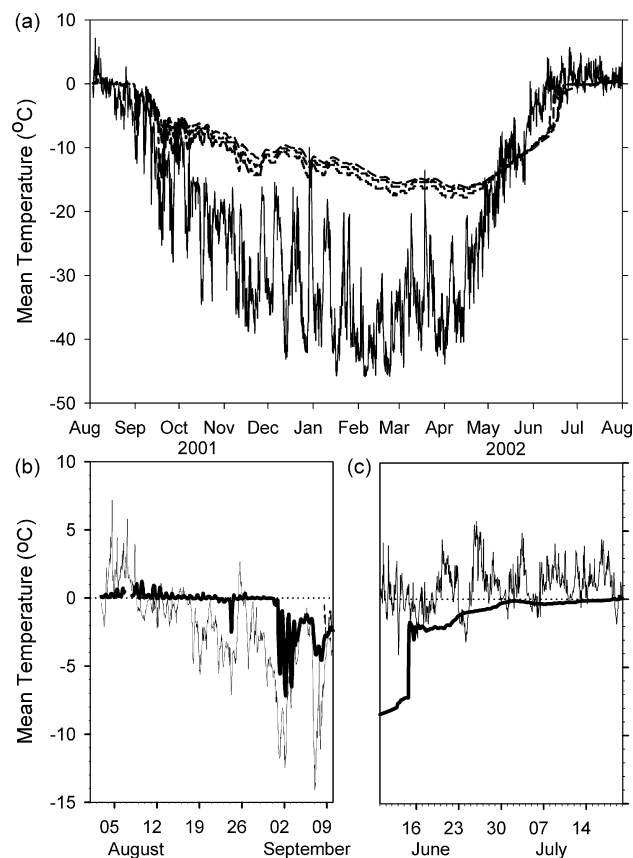


Figure 3. Mean surface air and microbial mat temperature. (a) Air temperature (solid line) versus the temperature within three microbial mats (dashed lines) between August 2001 and August 2002. (b) Air temperature (thin line) and microbial mat (thick line) temperature during freeze-up in 2001. (c) Air temperature (thin line) and microbial mat (thick line) temperature during thaw in 2002. (b and c) Dotted line indicates 0°C . Other microbial mat temperatures during freeze-up and thaw were similar to the one depicted, although timings varied (Table I)

Table I. Freeze-up and thaw dates of microbial mats on the Ward Hunt Ice Shelf. Freeze-up and thaw were operationally defined as the date when the microbial mat temperature remained below 0 °C for the winter and when it rose above 0 °C for the summer

Year	Freeze-up date	Thaw date	Period below 0 °C (days)
2001–02	31 August	18 July	321 ^a
	7 September	23 June	289
	7 September	23 June	285
2002–03	25 August	15 July	324
	26 August	24 July	332
	1 September	8 July	310
	1 September	11 July	313
	3 September	19 July	319
	7 September	6 July	302

^a The microbial mat shown in Figure 3b and c.

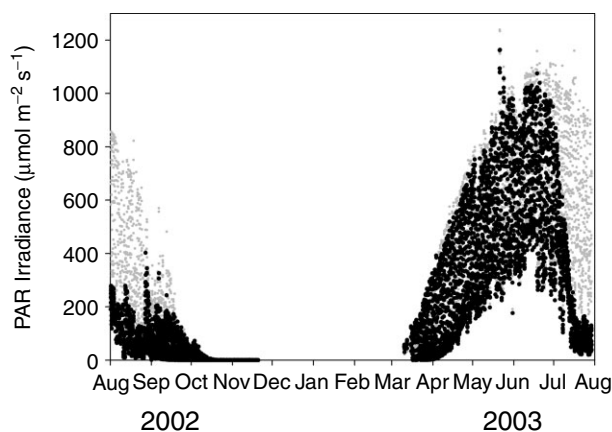


Figure 4. Downwelling (grey) and upwelling (black) PAR irradiance from August 2002 to August 2003. The drop in albedo at the site due to snowmelt can be clearly seen in July 2003. Note that data are missing between November and March

The surface albedo at the climate station was monitored between August 2002 and 2003. Major increases and decreases in albedo indicated the onset of substantial snow covering the microbial mats in September and the onset of snowmelt in July (Figure 4). Spot measurements of albedo over various surface cover types and sky conditions are given in Table II. The lowest albedos were measured over microbial mat and gravel, followed by water surfaces (especially those underlain by microbial mats or gravel), whereas snow consistently gave the highest albedos. Ice albedos were found to be variable, depending on the amount and distribution of candling and sediment cover. The albedo of some surfaces doubled between 100 and 150 cm above the surface in clear sky conditions due to the inclusion of highly reflective snow and ice into the sensor's field of view. However, there were no differences between measurements at 50 and 100 cm.

The underwater PAR sensor at the microbial mat surface recorded relatively high irradiances until early September 2001, when snow likely covered the frozen pond surface (Figure 5). Microbial mats in this particular meltwater pond were covered by ice until at least early September 2002, when the PAR sensor wire was severed. Microbial mats were often observed to be covered by ice with a 5 to 10 cm air space directly above them, which reduced irradiances to 1.2–56% of the incoming PAR (average: 15%), based on the July and August 2002 data presented in Figure 5. This ice covering usually candled over the summer

Table II. The albedo of various surface cover types on the Ward Hunt and Markham Ice Shelves^a

Substrate	Sky conditions			
	CLR	FG	BKN AC	SCT AC
Blue ice shelf lake	0.31 (0.005)	0.33 (0.001)	—	0.60 (0.02)
Sediment on ice	—	0.26 (0.002)	—	0.37 (0.01)
Gravel	—	0.09 (0.001)	—	—
Marine ice	—	—	—	0.77 (0.03)
Mat	0.23 (0.03)	0.10 (0.001)	0.16 (0.004)	—
Climate station area	—	—	—	0.56 (0.01)
Pond underlain by mat	0.30 (0.04)	0.11 (0.001)	0.09 (0.002)	—
Snow	0.89 (0.04)	0.76 (0.003)	0.67 (0.02)	—

^a Measurement heights were at 100 cm for clear sky conditions (CLR), fog (FG) and broken altocumulus (BKN AC) and 130 m for scattered altocumulus (SCT AC). Averages of 5 to 55 measurements (\pm SE).

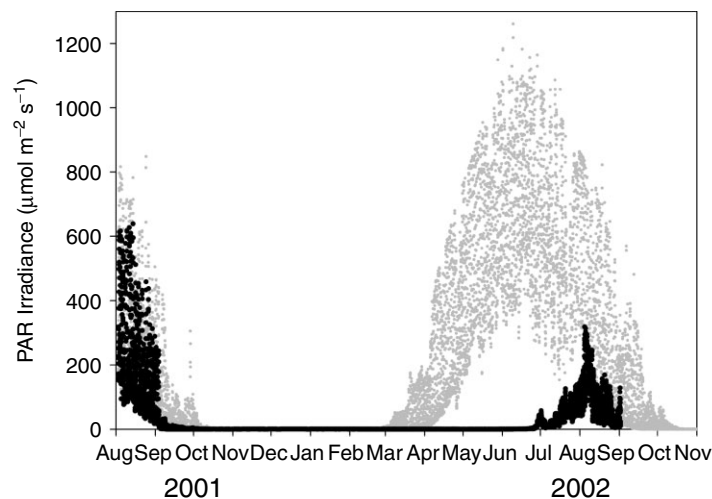


Figure 5. Downwelling (grey) PAR irradiance from August 2001 to August 2002 compared with irradiance 14 cm above the surface of a microbial mat (black). Initially, the microbial mat sensor was at the bottom of a meltwater pond (under 20 cm water). A drop in mat-level irradiance in early September 2001 suggests a snowfall event covered the frozen pond. The snow cover over this sensor candled in late July–August and the sensor wire was severed in early September 2002

months, and differences in PAR received under this covering may have been influenced by light piping through candled ice and solar zenith angles. The ice cover at nearby sites eventually collapsed, often exposing the microbial mats to direct sunlight.

Conductivity

From the topographical survey data and water depth measurements, the meltwater pond that contained the conductivity and temperature datalogger was 55 m² in planar surface area and 9.4 m³ in volume on 11 August 2002. At this point, the specific conductivity was 5.7 mS cm⁻¹, which was typical of other measurements taken during the 2002 melt season (Figure 6). After 398 freezing degree-days, the first Stowaway froze into the ice on 8 October 2002 at -0.32°C , and at this time the bottom-water specific conductivity was 10.2 mS cm⁻¹ and the volume of liquid water in the pond was estimated at 2.1 m³. The water surrounding the second Stowaway froze on 25 October 2002 after an additional 242 freezing degree-days. The pond water was then

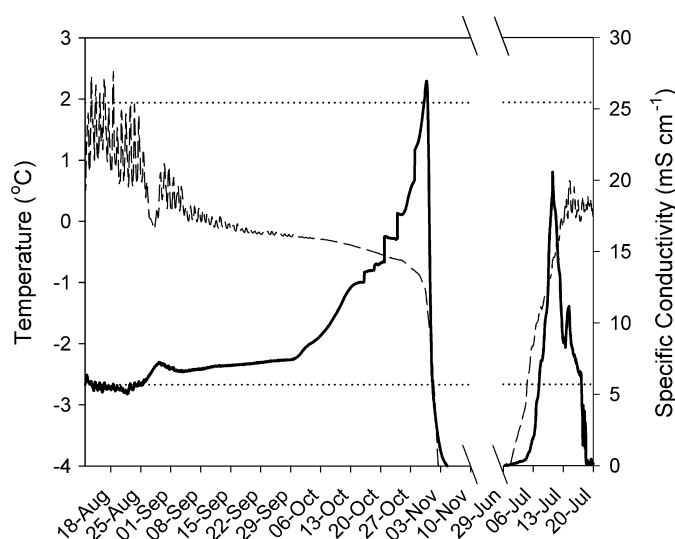


Figure 6. Freeze-up and thaw of a meltwater pond on the Ward Hunt Ice Shelf. Specific conductivity (solid line) and temperature (dashed line) every 30 min by a CTD logger installed at the bottom of the 9.4 m³ pond. Horizontal dotted lines indicate mean open-water conditions (measured from 23 July to 10 August 2002) for temperature (upper line) and specific conductivity (lower line). Note that ice inside the induction coil (torus) of the sensor caused a reduction in specific conductivity to a subzero reading over winter, which accounts for the rapid drop in conductivity at freeze-up and the rise in conductivity at thaw

an estimated 0.6 m³ and the bottom-water specific conductivity and temperature were 17.7 mS cm⁻¹ and -0.65 °C respectively. The pond froze completely on 30 October 2002, after a further 106 freezing degree-days, at the elevated conductivity of 27.0 mS cm⁻¹ and a temperature of -1.26 °C (Figure 6). We assume that the rapid drop in conductivity after this maximum is an artefact associated with the presence of ice within the torus. Conductivity was therefore reduced to a constant overwinter value of -1000 mS cm⁻¹ when ice completely encased the instrument (see also Hawes *et al.* (1999)).

Water column and microbial mat profiles

Vertical stratification in conductivity (Stratification Index >1.1) was observed in 54% of water column profiles taken on the Ward Hunt and Markham Ice Shelves. There was a significant difference between the stratification indices of ice-covered ponds versus non-ice covered ponds (Mann-Whitney $U = 204$, $p < 0.001$). The depth of each pond was also a suitable predictor of water column stratification when the ice cover was taken into account (Figure 7; multiple regression: Stratification Index = $-2.192 + (0.101d) + (3.772i)$, where d (cm) is depth of water column and i (= 1 or 0) is the presence of an ice cover, $R^2 = 0.35$, $p < 0.001$). Temperatures remained relatively constant throughout the water columns, with temperature rarely ~0.5 °C higher in the bottom waters (but in one instance increasing by 1 °C).

The microbial mat profiles of dissolved oxygen, pH and chloride typically showed little variation with depth and no evidence of discrete layering (Figure 8). There was a decrease in dissolved oxygen from the top of the mat to the bottom, consistent with the lack of photosynthesis and increased respiration in lower levels. The pH increased abruptly by two units at the bottom of one of the cryoconite mats. Chloride concentrations were the same with depth throughout the mats; however, chloride levels contrasted between mat types. Using an empirical relationship between ice shelf meltwater chloride levels and conductivity (Cond = $0.02436 + 0.00374 [\text{Cl}^-]$, $R^2 = 0.98$, $n = 25$, $p < 0.001$, where Cond is the conductivity (mS cm⁻¹) and $[\text{Cl}^-]$ is the chloride concentration (mg l⁻¹)), we estimate that the conductivities in the cryoconite hole and emergent mats differed by three orders of magnitude, from 0.05 ± 0.001 (cryoconite) to 64 ± 0.56 mS cm⁻¹ (emergent).

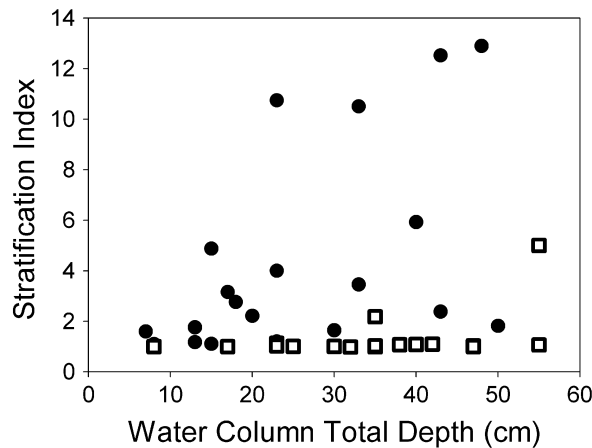


Figure 7. The relationship between stratification index (bottom water salinity divided by surface water salinity) and depth for ice-shelf meltwater ponds covered with ice (solid circle) and ice free (open square)

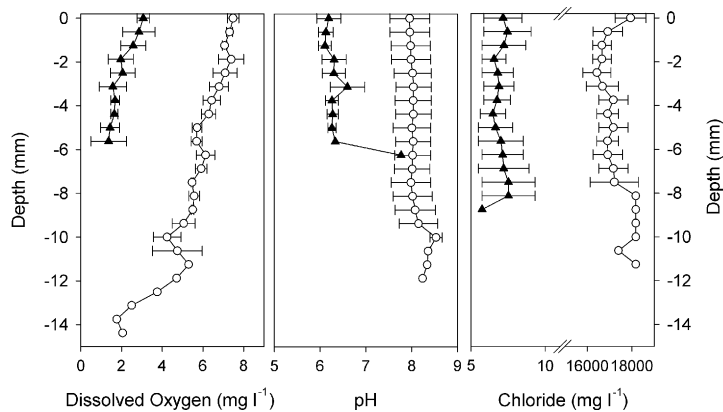


Figure 8. Microbial mat profiles of dissolved oxygen, pH and chloride for a mat overlain by 8 cm of water in a cryoconite hole (closed triangles) and an 'orange'-type mat not overlain by water (open circles). Averages with SE bars for three measurements

Nutrient concentrations and isotopic ratios

The differences between nutrient concentration in microbial mat pore water and the overlying water column are given in Table III. The mats had, on average, three orders of magnitude more DIC and $\text{NH}_4^+\text{-N}$ than the water column. The remaining variables were two orders of magnitude more concentrated in the microbial mat than in the overlying water. However, there was a high degree of variability in mat pore water nutrient concentration, particularly in the emergent mat, relative to the water column nutrient concentration. Consequently, the differences in nutrient concentrations between emergent and benthic mat pore water were not significant (one-way ranked ANOVA, Dunn's *post hoc* test, $P > 0.05$), while differences were significant between the benthic mat and the water column and between the emergent mat and the water column, with the exception of $\text{NH}_4^+\text{-N}$, $\text{NO}_3^-\text{-N}$ and SRP. Differences in nitrate and nitrite levels were not tested for significance owing to data being below detection limits.

The benthic mat pore water had a significantly higher CDOM content than the overlying water, as indicated by the analysis of a_{CDOM} values (Mann-Whitney test, $p = 0.008$). The McKnight ratio derived from fluorescence analysis indicated that CDOM composition was similar between the benthic mat pore water and overlying water (averages: 1.27 (SE = 0.12) and 1.29 (SE = 0.12) respectively). This ratio differentiates

Table III. Nutrient and CDOM concentrations of ice shelf meltwater and microbial mat pore water^a

Nutrient/constituent	Overlying water	Benthic mat	Emergent mat
DIC (mg l ⁻¹)	0.76 (0.051)	108 (25)	203 (116)
DOC (mg l ⁻¹)	0.26 (0.024)	60 (13)	165 (84)
<i>a</i> _{CDOM} (m ⁻¹)	0.32 (0.027)	7.23 (0.080)	—
TDN (mg l ⁻¹)	0.13 (0.020)	23 (7)	47 (35)
NH ₄ ⁺ -N (mg l ⁻¹)	0.064 (0.010)	10 (2)	12 (8)
NO ₃ ⁻ -N (mg l ⁻¹)	<0.006 (—) ¹	<0.19 (—) ⁴	4.13 (2.6)
NO ₂ ⁻ -N (mg l ⁻¹)	<0.001 (—) ⁵	<0.01 (—) ⁵	0.05 (0.04)
TDP (mg l ⁻¹)	0.006 (0.001)	0.45 (0.15)	0.48 (0.1)
SRP (mg l ⁻¹)	0.004 (0.001)	0.41 (0.07)	<0.25 (—) ²

^a Overlying water (*n* = 5), benthic mat (*n* = 5) and emergent mat (*n* = 4). Averages followed by standard error in parentheses. For mat pore waters, detection limits were variable and high due to the dilution of sample water with deionized water. If one or more samples in an average were not detected, then the limit of detection for those samples were averaged, averages are preceded by a less than symbol. Superscripts indicate how many samples were below detection.

between potential sources of organic matter, and in this case suggests that complex (typically terrestrially derived) fulvic acids were present in the samples (McKnight *et al.*, 2001).

Microbial mats had $\delta^{13}\text{C}$ values ranging from -22.30 to -16.63‰ (mean -18.95‰ , SE = 0.50‰ , *n* = 16) and $\delta^{15}\text{N}$ values ranging from -1.13 to 0.39‰ (mean -0.61‰ , SE = 0.35‰ , *n* = 16).

Snow accumulation and ablation

Snow accumulation and ablation were compared in a hollow versus a plateau near the climate station. The hollow was exposed at the time of sensor installation, with a microbial mat surface cover, whereas the plateau was composed of highly reflective ice that covered the mats. In the hollow, 0.30 ± 0.05 m of ice had ablated over the autumn (up to 24 November) and a net accumulation of 0.60 ± 0.10 m of snow occurred by 10 March 2003. At this time, the station resumed measurements with the return of the sun to power the solar panels. Between mid March and 18 July, the surface lowered by 0.65 ± 0.05 m (average spring–early summer surface lowering: 0.5 cm day⁻¹). On the plateau, 0.10 ± 0.05 m of ablation occurred between August and November and there was no net accumulation of snow (0.00 ± 0.05 m) between November and March. However, over the 4 month period from mid March to mid July, 1.35 ± 0.05 m of ice was lost (average spring–summer surface lowering: 1 cm day⁻¹).

Ice shelf ablation

Considerable ablation took place on the ice shelf during the study, in addition to morphological evolution and cover-type changes (Figure 2). Over 1 year (364 days), an average loss of 1.22 m of ice was recorded, which is equivalent to 1.10 m water equivalent. Over one-third (0.48 m) of this ablation occurred during the 2003 summer field season, 0.43 m was lost between the field seasons (at an average daily net loss of 0.13 cm day⁻¹) and the remainder was lost during the first 10 days of August 2002. During the 2002 field season, ice ablation was 2.9 cm day⁻¹ (SE = 0.26 cm day⁻¹) and the ablation rate was slightly higher (3.6 cm day⁻¹, SE = 0.15 cm day⁻¹) during the 2003 field season (Figure 9). However, it should be noted that the 2003 measurements were taken earlier than in 2002.

The ice shelf ablation stake network installed in 2004 allowed the measurements at the climate station to be compared with sites elsewhere. Between 2004 and 2005, the climate station site (cluster B) experienced an average of 1.04 m (SE = 0.17 m) of ablation (0.94 ± 0.15 m w. eq.). Ablation rates were significantly (*p* ≤ 0.05) higher at the marine ice sites (B, E: mean 0.75 m, SE = 0.19 m) versus the meteoric ice sites (A:

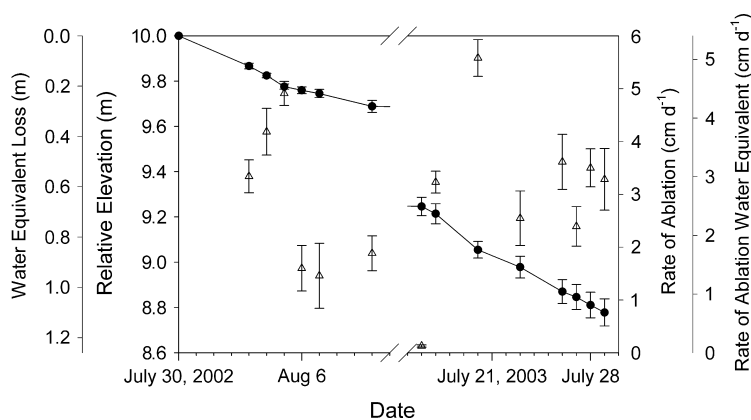


Figure 9. Ice ablation at the climate station site. Cumulative elevation loss and water loss (solid circles) and rates of ice- and water-equivalent ablation between site visits (open triangles). Averages and standard errors were calculated from six stakes from an arbitrary datum (10 m). Total ablation was 1.222 m (1.10 m w. eq.) over 364 days. The average rate of melt was 2.9 cm day^{-1} ($\text{SE} = 0.26 \text{ cm day}^{-1}$) during field season 2002 and 3.6 cm day^{-1} ($\text{SE} = 0.15 \text{ cm day}^{-1}$) during field season 2003

mean 0.42 m, $\text{SE} = 0.05 \text{ m}$; C: mean 0.22 m, $\text{SE} = 0.06 \text{ m}$; D: mean 0.22 m, $\text{SE} = 0.04 \text{ m}$) as indicated by a Holm–Sidak pairwise test (with the exception of the comparison between site A and E, $p = 0.06$).

Ice shelf topographic surveys

The topographic surveys in 2002 (Figure 10a) and 2003 (Figure 10b) indicated that a volume of 1270 m^3 of ice was lost over the 1103 m^2 area of the survey (Figure 10c). However, this estimate was partly offset by the presence of liquid water in the pond in 2002 (13.1 m^3) and in 2003 (39.6 m^3), bringing the ablation (including net liquid water advection) estimate down to 1243 m^3 (or $1.13 \text{ m} \approx 1000 \text{ kg m}^{-2}$).

The elevation range in 2002 was between 9.11 and 10.67 m, whereas in 2003 this range narrowed to between 8.15 and 9.63 m. The amount of surface lowering between 2002 and 2003 was 1.15 m on average and varied substantially across the site, from 0.43 to 2.01 m (Figure 10c). It is this differential surface lowering that could either act to exaggerate the existing topography (derived from the previous summer) or, conversely, could act towards inverting the relief between successive summers. If there were no variation in surface lowering between measurements, then the existing relative topography would be maintained. According to the inversion of relief hypothesis, differential albedo ensures that, by mid-summer, the high albedo cover types will remain at higher elevations (Table II; Figure 10). The exception to this general observation is that water, under the influence of gravity, will typically occupy the lowest elevations, forming ponds (e.g. Figure 10a, feature 1). Two four-level ranked ANOVAs confirmed that snow occupied the highest elevations in both 2002 and in 2003, followed by ice and then mat, with water occupying the lowest elevations (all pairwise differences were significant, Dunn's *post hoc* test, $p < 0.05$).

The principal driver of inversion of relief is the change in cover type from one summer to the next, which instigates differential ablation on the ice shelf. Higher than average surface lowering was measured (see Figure 10c) in areas covered with snow in 2002 that changed to mat cover (e.g. Figure 10a, feature 2), water cover (e.g. Figure 10a, feature 3), or ice (e.g. Figure 10a, feature 4). The erosive nature of water was also observed to lower mat- and snow-covered surfaces substantially (e.g. Figure 10a, features 5 and 6), suggesting that the hydrologic regime can also drive the surface lowering pattern. One of the changes in cover type associated with the least amount of surface lowering was water to snow cover (e.g. Figure 10a, feature 7), but low ablation also occurred in areas where cover type did not change (e.g. Figure 10a, features 1 and 8).

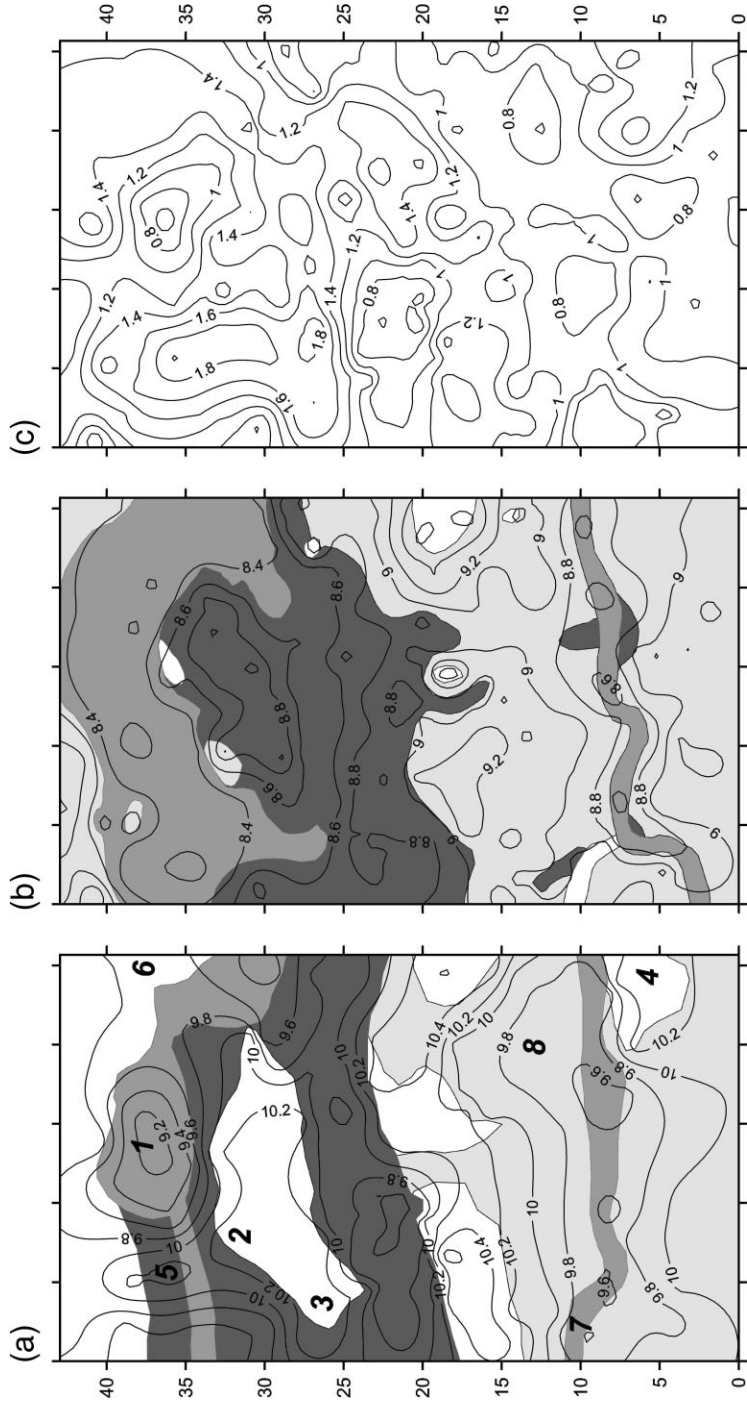


Figure 10. Ice shelf topography and ablation. (a) Topography on 4 August 2002, (b) topography on 27 July 2003 and (c) the difference between these surfaces (2002–03) represents the ice surface lowering. Cover types were assigned based on survey notes and photographs of the site. For Figure 10a and b, white: ice (often with surface dirt); grey: water (often underlain by microbial mat); dark grey: microbial mat; light grey: snow; light grey: ice (often with surface dirt); and surface lowering by microbial mat. The bold-italicized numbers in (a) are features referred to in the text. Distances, elevations and surface lowering are given in metres

DISCUSSION

Microbial mats were a significant component of overall cover at our study site on the Ward Hunt Ice Shelf. They were present over 23% (2002) to 27% (2003) of the survey site and, owing to methodological differences, these figures were higher than the mat cover values of 13 to 17% from a nearby point transect analysis (Mueller *et al.*, 2005b). The microbial mat environment contrasted markedly with bulk properties of the surrounding environment. This was observed with regard to both the climatology (irradiance and temperature) and the physical and chemical microenvironments (nutrient concentrations and conductivity). We observed an inversion of relief (Figure 2) and were able to quantify the extent of differential surface lowering (Figure 10).

Microhabitat climate

The temperature of the microbial mats over time influences metabolic processes and can determine the overall microbial mat productivity. The high specific and latent heat of the meltwater combined with the low albedo of both the mat and the meltwater (Table II) retard the freeze-up of the microbial mat relative to cumulative freezing degree-days (Figure 3b). Over winter, snow and ice insulated the microbial mats, thereby protecting them from extremely cold air temperatures, but also retarding melt-out in the spring. Metabolic activity has been shown to occur at temperatures down to -20°C , comparable to the minimum temperatures we recorded in the ice-shelf microbial mats (Rivkina *et al.*, 2000; Junge *et al.*, 2004), and it is likely that metabolic processes occur within the mats over winter, albeit at a minimal rate (Price and Sowers, 2004). The growth season, defined as the period of time when temperatures exceed $\sim 0^{\circ}\text{C}$, is equal to 8.7 weeks, or 16.7% of the year. Given the moderately high rates of primary production within the microbial mats ($64\text{ mg m}^{-2}\text{ h}^{-1}$ of carbon; Mueller *et al.*, 2005a), interannual variability in the growth season is potentially important with regard to overall production over the entire ice shelf area that contains suitable microbial habitat (83 km^2 ; Mueller *et al.*, 2005b).

The snow accumulation and underwater (near-mat) PAR measurements suggest that microbial mats at the bottom of depressions can remain covered by iced firn or snow over an entire melt season, which supports the 'inversion of relief' hypothesis. The shading of the overlying snow reduces PAR levels to 15% of ambient; however, this reduction in irradiance does not likely affect the productivity of microbial mats, owing to their demonstrated ability to acclimate to reduced irradiances both on the Ward Hunt Ice Shelf (Mueller *et al.*, 2005a) and the McMurdo Ice Shelf in Antarctica (Hawes *et al.*, 1999).

Conductivity

The high conductivity caused by brine exclusion during freezing (Figure 6) would probably have affected photosynthesis within the microbial mat, since primary productivity in these mats was found to be 50% lower at 29 mS cm^{-1} than at 0.1 and 2.9 mS cm^{-1} (Mueller *et al.*, 2005a). However, the heterotrophic bacterial productivity possibly suffered more from high conductivities, since experimental evidence shows a 3.4-fold reduction in heterotrophic bacterial production across this same range (Mueller *et al.*, 2005a). In contrast Hawes *et al.* (1999) found that mat photoautotrophs on the McMurdo Ice Shelf readily acclimated to even higher salinities than we observed.

The relatively high conductivity measured here at the onset freezing and melt was also observed in Brack Pond on the McMurdo Ice Shelf (Hawes *et al.*, 1999). Freeze concentration was by a factor of 1.5 times relative to Brack Pond summer conductivity, 6 times for Fresh Pond (also on the McMurdo Ice Shelf) and 4.7 times for the pond in this experiment. The solute concentration at freezing depends greatly on the position of the conductivity sensor and the bathymetry of the pond, as well as the freezing rate, which determines the potential exclusion of salts from the growing ice cover. The heat capacity of this relatively large volume of water ensured that the microbial mats in this microenvironment remained unfrozen long after other microbial mats in this study were frozen. Freezing of this particular pond was relatively slow, allowing for the rejection of a large proportion of the solutes within the water column. Thawing occurred far more rapidly in June (note the abrupt rise in temperature in Figure 6) and the specific conductivity was not as high (maximum

of 20.6 mS cm^{-1}) relative to the conductivity during freeze-up. This is probably due to the channelling of brine downwards away from the sensor at some point after 30 October; alternatively, it could be due to the percolation of low-salinity meltwater from above prior to the complete thawing of the sensor.

Water column and microbial mat profiles

The observed water column stratification has implications for meltpond biology, as it leads to a greater habitat differentiation between the water column and the benthic microbial mats. The stratification of small to medium meltponds on the Ward Hunt Ice Shelf likely occurs over time in the absence of wind mixing. The presence of ice covers and the depth of meltholes both act to reduce or prevent wind mixing and, therefore, are significant ($p < 0.01$) predictors of the stratification index (Figure 7). The wind speed over the period when measurements took place was under 5 m s^{-1} , except for the afternoon of 4 August ($< 10 \text{ m s}^{-1}$). All the ice-covered meltponds in the lower right quadrant of Figure 7 (depth $> 30 \text{ cm}$, Stratification Index < 8) were measured after this wind event. It is possible that these ice covers formed after wind-induced mixing and the water columns had not completely re-stratified prior to measurement. The relative constancy of temperature throughout the water column suggests that solar heating of benthic material does not increase the temperature of bottom water, but rather melts ice. This is not the case in ponds on the McMurdo Ice Shelf, which have a very thick ($\sim 30 \text{ cm}$) sediment cover that insulates the subjacent ice (Issaac and Maslin, 1991). Bottom waters there regularly exceed 5°C and can be as warm as 11°C due to intense density stratification (Hawes *et al.*, 1999).

The electrode profiles of dissolved oxygen, pH and chloride of the mats on the Ward Hunt Ice Shelf highlight the differences between microhabitats. The high chloride concentration in the emergent orange mats is likely to reflect evaporative concentration of salts within the mat pore water. This high salinity within the emergent mats would reduce photosynthesis, relative to cryoconite holes, based on available bioassay data, yet it might favour photoautotrophs, since photosynthesis may not decrease as much as heterotrophic productivity (Mueller *et al.*, 2005a). Furthermore, the emergent microbial mats are expected to be warmer than those in cryoconite holes, which have been noted to increase photosynthetic but not heterotrophic productivity (Mueller *et al.*, 2005a). Therefore, the emergent mats may be a microhabitat that is conducive to the accumulation of organic matter due to minimal decomposition rates. Both types of microbial mat show a decrease in dissolved oxygen concentration, which suggests that the lower mat receives less light than the surface and is a zone where respiration is greater than photosynthesis. It was noted that the pH increased dramatically if the probe touched the ice at the bottom of the mat, and it is possible that the bottom-most pH value in the cryoconite hole may be an artefact (Figure 8). Aside from this, the conductivity and pH profiles were featureless, which may reflect the loosely cohesive character of the mat. In this type of microbial mat there were no macroscopic indications of defined strata, with the exception of an orange surface layer up to $200 \mu\text{m}$ thick. This contrasts with a more layered mat type found in nearby Ward Hunt Lake on Ward Hunt Island (Villeneuve *et al.*, 2001; Bonilla *et al.*, 2005).

Nutrient concentrations and isotopic ratios

The relatively high concentration of nutrients within the microbial mats further illustrates how the microbial mat microenvironment is dissimilar from the rest of the ice shelf habitat. High microbial mat nutrient concentrations have been found in other locations, including Ward Hunt Lake, adjacent to the Ward Hunt Ice Shelf (Villeneuve *et al.*, 2001), and the McMurdo Ice Shelf (Vincent *et al.*, 1993). A comparison of the chloride concentrations in emergent ($17\,000 \text{ mg l}^{-1}$) and benthic mats (7 mg l^{-1} ; Figure 8) and the average water column chloride concentration on the Ward Hunt Ice Shelf (119 mg l^{-1} ; Mueller *et al.*, 2005b) point to concentration of this conservative tracer in the emergent mats but not in the benthic mats. It is plausible that evapo-concentration may be partially responsible for elevated nutrient and chloride concentrations in emergent mats, in contrast with benthic mats, where the process of nutrient concentration may be biologically mediated or influenced by the aeolian sediment flux.

It has been shown that benthic microbial mats can be effectively isolated from the water column nutrients due to a diffusion-limited boundary layer, and this may lead to deficiencies in DIC or other nutrients (Jørgensen, 1994), which would be exacerbated by water column stratification. The high nutrient and DIC concentration within microbial mat pore water on the Ward Hunt Ice Shelf suggests that this microenvironment is carbon and nutrient replete. This view has been experimentally confirmed with microbial mat nutrient enrichment experiments in nearby Ward Hunt Lake (Bonilla *et al.*, 2005). Furthermore, there is no isotopic evidence of substantial carbon limitation on the Ward Hunt Ice Shelf, as seen in benthic communities elsewhere (Turner *et al.*, 1994; Lawson *et al.*, 2004), although the water column and microbial mat pore-water $\delta^{13}\text{C}$ in DIC remain unknown. The near-zero $\delta^{15}\text{N}$ signatures suggest that the nitrogen may be fixed by heterocystous cyanobacteria (Goericke *et al.*, 1994), which are known to exist within these mats (Mueller *et al.*, 2005b). It is also possible that the marine-derived ice in this locality contained seawater nitrate (+7.0‰; Wada *et al.*, 1981) and that the fractionation during uptake (Goericke *et al.*, 1994: table 9.4) led to an ultimate signature near 0‰ in the biomass.

The McKnight ratio indicates that the CDOM within the microbial mats and in the pond water was either composed of complex molecules or is allochthonous (McKnight *et al.*, 2001). Terrestrial vegetation debris, such as *Salix arctica* leaves, has occasionally been observed within the ice shelf microbial mats, but this input is unlikely to be large. The presence of other water-soluble compounds, such as extracellular polymeric substances (EPS) and oligosaccharide mycosporine-like amino acids, which are prevalent in the microbial mat and may mix into the water column, may be responsible for such low McKnight ratios. Similarly, cellular contents, such as DNA and amino acids, may be released into the water column due to cyanophage activity within these mats (Short and Suttle, 2005). An alternate hypothesis derived from observations of lake ice (Belzile *et al.*, 2002) is that complex fulvic acids may be differentially freeze-concentrated while less complex CDOM molecules would be incorporated within the ice and may be flushed out during spring melt.

Ice shelf surface mass balance

Past studies note the high interannual and spatial variability of snow cover on the Ward Hunt Ice Shelf (Hattersley-Smith and Serson, 1970; Serson, 1979). Using an assumed snow bulk density of 0.31 g cm^{-3} (Braun *et al.*, 2004) and our two snow depth measurements on the Ward Hunt Ice Shelf for the winter of 2002–3, we calculated a minimum accumulation of between 0.00 ± 0.015 and 0.186 ± 0.031 m w. eq. This compares with mean net winter surface accumulation values from previous Ward Hunt Ice Shelf data (mean 0.10 to 0.17 m w. eq., individual pole range 0.02 to 0.44 m w. eq.; Serson, 1979).

Our main study site was located in an area of exposed marine ice and was locally different from the main ice shelf, where meteoric ice was observed at the surface. Marine ice covers 29% of the surface of the Ward Hunt Ice Shelf, 86% of Markham Ice Shelf and contains large amounts of sediment and microbial mats (Mueller *et al.*, 2005b). Braun *et al.* (2004) determined that the year 2002–03 had one of the largest negative mass balance on record for the Ward Hunt Ice Shelf (0.54 m w. eq.), from measurement of two ablation stakes in an area of meteoric ice to the east of Ward Hunt Island. The annual (net) surface mass balance recorded from our site for 2002–03 is two times higher than the ablation reported by Braun *et al.* (2004), and higher than past surface mass balance measurements on the Ward Hunt Ice Shelf. Previous measurements from individual poles ranged from 0.81 m of net accumulation to 1.04 m of net ablation (annual means ranged from +0.095 to –0.256 m w. eq.) between 1966 and 1976 (Serson, 1979). The difference in ablation between the meteoric and marine ice areas of the Ward Hunt Ice Shelf was also illustrated by data from five separate sites between 2004 and 2005. The original ablation network (positioned near site A in 1966) was not intended to be spatially representative of the entire ice shelf (Braun *et al.*, 2004). Nevertheless, our results indicate that ablation in marine ice areas can be twice as much as ablation at this original measurement site and over four times higher than in other meteoric ice areas (i.e. clusters C and D). We do not suggest that the microbial mats that are abundant in marine ice areas are solely responsible for the enhanced ablation that we observed, although they likely contribute to it. Rather, we suggest that marine ice areas on the Ward Hunt Ice Shelf may be partially

instigated by local climatological differences from meteoric ice areas. For example, Walker Hill (450 m a.s.l.) on Ward Hunt Island is a topographic barrier, which often disrupts layers of low-lying fog and stratus above our main study site, allowing direct solar radiation to penetrate to the ice surface (personal observation). The lack of net accumulation in marine ice areas keeps microbial mats at or near the ice surface, where they contribute to the overall surface lowering and to the cyclical inversion of relief via their relatively low albedo.

It is known that marine ice areas on the Ward Hunt Ice Shelf are replenished by the basal freeze-on of seawater (Crary, 1960). This is evidenced by the presence of marine invertebrates on the surface of the ice shelf that made their way through the ice via this ablation mechanism (Debenham, 1920). Using the 2002–03 ice ablation as a marine ice zone maximum rate and assuming an ice shelf thickness of 40 m, then marine sediments and invertebrates could be lifted to the surface of the ice shelf in as little as 33 years.

The Ward Hunt Ice Shelf is not glacially fed, and its surface topography does not vary more than 7.5 m (Jeffries *et al.*, 1990). Therefore, the concept of equilibrium line altitude (ELA) does not apply in the vertical sense to surface mass balance. Rather, it exists horizontally, but on long time scales (greater than decadal), between regions of perennial surface mass loss (marine ice) and regions where surface accumulation takes place (meteoric ice). If the surface mass balance of the Ward Hunt Ice Shelf remains negative, then this 'long-term horizontal equilibrium zone' will encroach on the meteoric ice regions, exposing more marine ice at the surface, as the overlying meteoric ice ablates. To compare with a characteristic glacial system in the High Arctic, the average (1960–2001) ELA for the White Glacier on Axel Heiberg Island (79°N) was 1100 m a.s.l. and the elevation where the average net loss was equivalent to our 2002–03 measurement was at 500 m a.s.l. (the terminus of the White Glacier is currently near 56 m a.s.l.; Cogley, 2002).

Inversion of relief and the role of microbial mats

The observations obtained in this study allow an explicit test of the inversion of relief hypothesis. Two predictions follow from this hypothesis, and must be achieved to demonstrate that inversion of relief occurred on the ice shelf. First, the hypothesis predicts a dynamic pattern of change over horizontal space, with a substantial shift in surface cover type between summers. Second, the hypothesis also predicts a consistency of vertical zonation that is associated with relative albedo and gravitational effects. Specifically, bright snow should be higher than less reflective ice, which in turn should be at a higher elevation than dark-coloured mat, whereas water will drain downwards and will occupy the lowest elevations.

At our climate station site between surveys, the cover type changed at 42% of the nodes. Although conditions were not conducive for a complete inversion of relief over this period (compare Figure 2b and c with Figure 2a and b), this change is substantial and is consistent with the first prediction of spatial dynamics. Using the data where cover class changed between surveys, the 2003 elevation data were grouped according to the cover type in 2003. The highest average elevation was for snow (9.1 m), followed by ice (8.9 m), then mat (8.8 m) and finally water (8.4 m). All pairwise comparisons between cover-type elevations were significantly ($p < 0.05$) different with the exception of snow versus ice, which may reflect the low number of observations for snow in 2003. In addition, the same elevational zonation was identified in 2002 from the nodes where cover type changed. The highest average elevation for 2002 was snow (10.1 m), followed by ice (9.9 m), then mat (9.8 m) and finally water (9.6 m), consistent with the second prediction. All pairwise comparisons between cover-type elevations were significantly ($p < 0.05$) different with the exception of ice versus mat. The only way that this elevational zonation can be preserved between two consecutive summers, despite the cover-type change between measurements, is through the process of relief inversion as described by Smith (1961). We conclude that inversion of relief was occurring at our study site between the summers of 2002 and 2003, and influenced just under half of the icescape.

One factor that encourages the inversion of relief in this ice shelf environment is the tendency for microbial mats to slump downwards towards lower elevations, particularly when ice slopes become critically steep. The high salt content in emergent mats (Figure 8) will intensify ice melting, thereby lubricating the interface between the microbial mat and ice. Slumping of microbial mats in a cohesive manner is likely enhanced by

the biosynthesis of EPS. This class of compounds acts to bind organisms to sediments, as well as to each other, and is an important component of microbial mats (Yallop *et al.*, 1994; Stal, 2003). Microbial mat EPS and the trichomes of filamentous cyanobacteria also act to trap and stabilize sediments, thereby preventing their dispersion across the ice shelf environment by aeolian or hydrological processes. Ward Hunt Ice Shelf mats contain up to 24% organic matter (D. R. Mueller, unpublished data) and are loosely cohesive, indicating the presence of EPS. Based on this evidence, we conclude that the EPS-stabilized microbial mats are likely to behave differently than purely abiotic sediments and will thereby have a stronger influence on the evolution of the ice shelf surface morphology than sediments alone.

The inversion of relief on ice appears to be sensitive to microbial mat cover and thickness. In the absence of mats or sediments there is no relief inversion and the existing topography is maintained or amplified. For example, old hummocks on a sediment-free multiyear floe in the Arctic Ocean (81.5 to 84 °N) were shown to have 39% less ablation than flat areas on the floe, suggesting that these features are self-perpetuating (Koerner, 1973). This is also the case for areas of meteoric ice on the Ward Hunt Ice Shelf, which are 7% covered by microbial mats (Mueller *et al.*, 2005b). Ridges in these areas have slightly lower net ablation than the troughs (Serson, 1979). When a thin layer of sediment or microbial mat is present, conditions favour the inversion of relief. On the other hand, excessive inorganic debris can impede ice ablation due to insulation of the ice from both radiative and aeolian forcing (Schraeder, 1968). For example, in marine ice areas on the Ward Hunt and Markham Ice Shelves, microbial mats can accumulate to thicknesses in excess of 2 cm, which insulates the underlying ice and, consequently, the surface morphology includes features such as dirt cones (Sharp, 1949; Wilson, 1953). This provides an additional mechanism of biotic control of ice relief. Conversely, the inversion of relief is likely restricted to relatively thin mats that are less than the thickness required to insulate the underlying ice fully.

CONCLUSIONS

The temperature, radiation, conductivity and nutrient data reported here show that the microbial mat microhabitat differs substantially from the bulk properties of the ice shelf ecosystem. In some respects these microhabitats may be more clement for biological processes, with longer melt seasons, warmer overwinter temperatures and higher nutrient concentrations than the surroundings. However, depending on their location and time of year, microbial mats may experience sustained periods of low or high irradiance stress, and may be subjected to osmotic stress due to water column stratification, evaporation or freeze concentration.

Microbial mats can affect the physical ice shelf environment in such a way that favours their ongoing growth and ecological success. Mechanisms of physical–biotic coupling reduce mat albedo and include the trapping of sediments within the microbial mat matrix, the EPS stabilization of this matrix to prevent sediment redistribution, and mass-slumping of cohesive EPS-permeated mat towards water-filled depressions on the ice shelf surface, consistent with an inversion of relief. The accelerated ablation associated with the latter in marine ice areas of ice shelves benefits the microbial community by entraining more marine sediments and nutrients from below while also inhibiting surface mass balance gains and the accumulation of light-screening surface snow and ice.

ACKNOWLEDGEMENTS

We acknowledge financial support from the Natural Sciences and Engineering Research Council (Discovery Grant to WFV and Graduate Scholarship to DRM), the Canada Research Chair in Aquatic Ecosystem Studies, the Network of Centres of Excellence program ArcticNet, and the Northern Scientific Training Program. Logistical support was supplied by the Polar Continental Shelf Project (this is PCSP/ÉPCP publication number 01005). Field assistance was provided by Katie Breen, Sébastien Roy, Jeffrey Kheraj, Denis Sarrazin, Alexandra Pontefract, Eric Botton, Carsten Braun and Vicki Sahanatian. We thank Ladd Johnson and Wayne

Pollard for the loan of equipment and Christine Martineau and Marie-Josée Martineau for laboratory assistance. We acknowledge the helpful comments of Dominic Hodgson and two anonymous reviewers.

REFERENCES

- Adams WP. 1966. *Studies of ablation and run-off on an Arctic glacier*. PhD thesis, Department of Geography, McGill University, Montreal.
- Belzile C, Gibson JAE, Vincent WF. 2002. Colored dissolved organic matter and dissolved organic carbon exclusion from lake ice: implications for irradiance transmission and carbon cycling. *Limnology and Oceanography* **47**: 1283–1293.
- Blanck E, Poser H, Oldershausen E. 1932. Über Kryokonitvorkommnisse im ostgrönländischen Packeis und ihre chemische Zusammensetzung. *Chemie der Erde* **7**: 434–440.
- Bonilla S, Villeneuve V, Vincent WF. 2005. Benthic and planktonic algal communities in a high arctic lake: Pigment structure and contrasting responses to nutrient enrichment. *Journal of Phycology* **41**: 1120–1130. DOI: 10.1111/j.1529-8817-2005-00154-x.
- Brandt B. 1931. Kryokonit auf Flußeis in Mitteleuropa. *Zeitschrift für Gletscherkunde* **19**: 317–320.
- Braun C, Hardy DR, Bradley RS, Sahanatian V. 2004. Surface mass balance of the Ward Hunt Ice Rise and Ward Hunt Ice Shelf, Ellesmere Island, Nunavut, Canada. *Journal of Geophysical Research—Atmospheres* **109**: D22 110. DOI: 10.1029/2004JD004560.
- Cogley JG. 2002. *Mass balance of Axel Heiberg Island glaciers*. Trent University, Peterborough, ON; www.trentu.ca/geography/glaciology.2003/glaciology.htm [31 May 2005].
- Crary AP. 1960. Arctic ice islands and ice shelf studies, part II. *Arctic* **13**: 32–50.
- Debenham F. 1920. A new mode of transportation by ice: the raised marine muds of South Victoria Land. *Quarterly Journal of the Geological Society* **75**: 51–76.
- Fountain AG, Tranter M, Nylen TH, Lewis KJ, Mueller DR. 2004. Evolution of cryoconite holes and their contribution to melt-water runoff from glaciers in the McMurdo Dry Valleys, Antarctica. *Journal of Glaciology* **50**: 35–45.
- Goericke R, Montoya JP, Fry B. 1994. Physiology of isotopic fractionation in algae and cyanobacteria. In *Stable Isotopes in Ecology and Environmental Science*, Lajtha K, Michener RH (eds). Blackwell Scientific: Boston; 187–221.
- Hattersley-Smith G, Serson H. 1970. Mass balance of the Ward Hunt Ice Rise and Ice Shelf: a 10 year record. *Journal of Glaciology* **9**: 247–252.
- Hawes I, Smith R, Howard-Williams C, Schwarz AM. 1999. Environmental conditions during freezing, and response of microbial mats in ponds of the McMurdo Ice Shelf, Antarctica. *Antarctic Science* **11**: 198–208.
- Issaac P, Maslin D. 1991. *Physical Hydrology of the McMurdo Ice Shelf*. New Zealand Antarctic Research Programme: Christchurch.
- Jeffries MO. 2002. Ellesmere Island ice shelves and ice islands. In *Satellite Image Atlas of Glaciers of the World: North America*, Williams RS, Ferrigno JG (eds). United States Geological Survey: Washington, DC; J147–J164.
- Jeffries MO, Krouse HR, Sackinger WM, Serson HV. 1990. Surface topography, thickness and ice core studies of multiyear landfast sea ice and Ward Hunt Ice Shelf, Northern Ellesmere Island, N.W.T. In *Canada's Missing Dimension: Science and History in the Canadian Arctic Islands*, Harington CR (ed.). Canadian Museum of Nature: Ottawa; 229–254.
- Jørgensen BB. 1994. Diffusion processes and boundary layers in microbial mats. In *Microbial Mats: Structure, Development and Environmental Significance*, Stal LJ, Caumette P (eds). Springer-Verlag: Berlin; 243–254.
- Junge K, Eicken H, Deming JW. 2004. Bacterial activity at –2 to –20 degrees C in Arctic wintertime sea ice. *Applied and Environmental Microbiology* **70**: 550–557. DOI: 10.1128/AEM.70.1.550–557.2004.
- Kirk JTO. 1983. *Light and Photosynthesis in Aquatic Ecosystems*. Cambridge University Press: Cambridge.
- Koerner RM. 1973. The mass balance of the sea ice of the Arctic Ocean. *Journal of Glaciology* **12**: 173–185.
- Lawson J, Doran PT, Kenig F, Des Marais DJ, Priscu JC. 2004. Stable carbon and nitrogen isotopic composition of benthic and pelagic organic matter in lakes of the McMurdo Dry Valleys, Antarctica. *Aquatic Geochemistry* **10**: 269–301.
- Leslie A. 1879. *The Arctic Voyages of A.E. Nordenskjöld*. MacMillan: London.
- McIntyre NF. 1984. Cryoconite hole thermodynamics. *Canadian Journal of Earth Sciences* **21**: 152–156.
- McKnight DM, Boyer EW, Westerhoff PK, Doran PT, Kulbe T, Andersen DT. 2001. Spectrofluorometric characterization of dissolved organic matter for indication of precursor organic material and aromaticity. *Limnology and Oceanography* **46**: 38–48.
- Mueller DR, Vincent WF, Bonilla S, Laurion I. 2005a. Extremotrophs, extremophiles and broadband pigmentation strategies in a High Arctic ice shelf ecosystem. *FEMS Microbiology Ecology* **53**: 73–87. DOI: 10.1016/j.femsec.2004.11.001.
- Mueller DR, Vincent WF, Jeffries MO. 2005b. Environmental gradients, fragmented habitats and microbiota of a northern ice shelf cryoecosystem. *Arctic, Antarctic, and Alpine Research* submitted for publication.
- Price PB, Sowers T. 2004. Temperature dependence of metabolic rates for microbial growth, maintenance, and survival. *Proceedings of the National Academy of Sciences* **101**: 4631–4636. DOI: 10.1073/pnas.0400522101.
- Rivkina EM, Friedmann EI, McKay CP, Gilichinsky DA. 2000. Metabolic activity of permafrost bacteria below the freezing point. *Applied and Environmental Microbiology* **66**: 3230–3233.
- Schraeder RL. 1968. *Ablation of Ice Island ARLIS II, 1961*. MSc thesis, Department of Geology, University of Alaska, College, AK.
- Serson HV. 1979. *Mass balance of the Ward Hunt Ice Rise and Ice Shelf: an 18-year record*. Defence Establishment Pacific, Victoria, Victoria, BC.
- Sharp RP. 1949. Studies of superglacial debris on valley glaciers. *American Journal of Science* **247**: 289–315.
- Short C, Suttle C. 2005. Nearly identical bacteriophage structural gene sequences are widely distributed in both marine and freshwater environments. *Applied and Environmental Microbiology* **71**: 480–486. DOI: 10.1128/AEM.71.1.480–486.2005.
- Smith DD. 1961. Sequential development of surface morphology on Fletcher's Ice Island, T-3. In *Geology of the Arctic*, Raasch GO (ed.). University of Toronto Press: Toronto; 896–914.
- Smith DD. 1964. Ice lithologies and structure of Ice Island ARLIS II. *Journal of Glaciology* **5**: 17–38.

- Stal L. 2003. Microphytobenthos, their extracellular polymeric substances, and the morphogenesis of intertidal sediments. *Geomicrobiology Journal* **20**: 463–478. DOI: 10.1080/01490450390237157.
- Takeuchi N, Kohshima S, Fujita K. 1998. Snow algae community on a Himalayan glacier, Glacier AX010 east Nepal: relationship with glacier summer mass balance. *Bulletin of Glacier Research* **16**: 43–50.
- Turner MA, Howell ET, Robinson GGC, Campbell P, Hecky RE, Schindler EU. 1994. Roles of nutrients in controlling growth of epilithon in oligotrophic lakes of low alkalinity. *Canadian Journal of Fisheries and Aquatic Sciences* **51**: 2784–2793.
- Villeneuve V, Vincent WF, Komárek J. 2001. Community structure and microhabitat characteristics of cyanobacterial mats in an extreme High Arctic environment: Ward Hunt Lake. *Nova Hedwigia, Beiheft* **123**: 199–224.
- Vincent WF, Castenholz RW, Downes MT, Howard-Williams C. 1993. Antarctic cyanobacteria: light, nutrients, and photosynthesis in the microbial mat environment. *Journal of Phycology* **29**: 745–755.
- Wada E, Shibata R, Torii T. 1981. ¹⁵N abundance in Antarctica: origin of soil nitrogen and ecological implications. *Nature* **292**: 327–329. DOI: 10.1038/292327a0.
- Wilson JW. 1953. The initiation of dirt cones on snow. *Journal of Glaciology* **2**: 281–287.
- Yallop ML, Dewinder B, Paterson DM, Stal LJ. 1994. Comparative structure, primary production and biogenic stabilization of cohesive and noncohesive marine-sediments inhabited by microphytobenthos. *Estuarine Coastal and Shelf Science* **39**: 565–582.